

Andrew Streitwieser

## Ion pair aggregates and reactions; experiment and theory

Received: 10 May 2005 / Accepted: 28 September 2005 / Published online: 9 December 2005  
© Springer-Verlag 2005

**Abstract** Two methods have been developed for determining the aggregation equilibrium constants of lithium enolates based on the change in UV-vis spectrum with concentration and the effect of aggregation on proton-transfer equilibria. Dimers and tetramers are common. Substitution  $\alpha$  to the carbonyl group generally reduces aggregation. Kinetic studies show that  $S_N2$  alkylations generally occur with the monomers, even in the presence of large amounts of aggregate. The qualitative chemistry is well modeled by ab initio computations at the HF level with modest basis sets; in these studies solvation is modeled by a combination of coordination of lithium cation with an ether oxygen and the electrostatic interaction of the resulting dipoles and quadrupoles with the solvent dielectric continuum.

**Keywords** Aggregation · Alkylation · Equilibrium constant · Acidity · Molecular orbital

### Introduction

Modern organic syntheses frequently take place in organic solvents in which the active reagents are often present as ion pairs and aggregates. Relatively little research has been done on the equilibrium constants for aggregate formation and their reactivities. Much of my research during the past

decade or so has been devoted to the study of aggregates of lithium and cesium enolates. In this review, I will emphasize lithium enolates and our methods for determining aggregation equilibrium constants and reactivities, the experimental results and our initial approaches in modeling this chemistry with ab initio molecular orbital theory at a modest level, RHF with the 6-31+G\* basis set.

Preformed lithium enolates are important reagents in organic synthesis because they can be alkylated by  $S_N2$  reactions with alkyl halides and sulfonates and they undergo aldol addition reactions with carbonyl compounds; both are useful routes to generating new carbon-carbon bonds [1–5]. These enolates have long been known to be aggregated in ethereal solutions as well as in the solid state [6], and such aggregates have been suggested to be involved in reactions. [7] Actual evidence for the involvement of lithium enolate aggregates, however, is sparse. The problem is that at normal temperatures the equilibria among aggregates are rapid, giving rise to a classic Curtin–Hammett situation (Scheme 1) [8].

The total rate of reaction is given by Eq. 1 in which the aggregation equilibrium constants are defined relative to the ion-pair monomer whose concentration is  $[M]$ . It is possible that even though an aggregate dominates the equilibrium, the rate constant of a monomer could be sufficiently high that most of the flux of reaction occurs through the monomer. Indeed, this is what we have generally found.

---

Dedicated to Professor Dr. Paul von Ragué Schleyer on the occasion of his 75th birthday

This review is based on the fifth annual Paul vR Schleyer Lecture presented at Professor Schleyer's 75th birthday symposium, Athens GA, Feb 26, 2005. Carbon Acidity 123. For no. 122 see Streitwieser A, Kaufman MJ, Bors DA, MacArthur CA, Murphy JT, Guibe F, Arkivoc (2005) (vi) 200–210

A. Streitwieser (✉)  
Department of Chemistry, University of California,  
Berkeley, CA 94720-1460, USA  
e-mail: astreit@berkeley.edu  
Tel.: +1-510-6422205  
Fax: +1-510-8416072

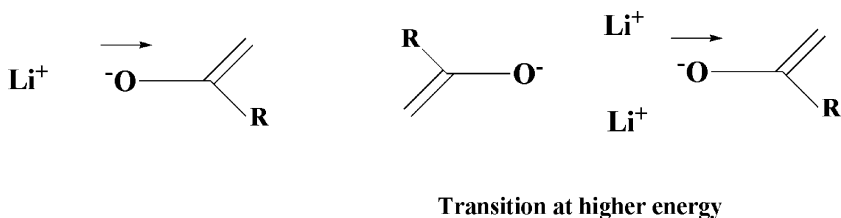
$$\text{Rate} = \sum k_n K_n [M]^n \quad (1)$$

---

### Methods and results

In order to establish the relative roles of monomer and aggregate in reactivity, it is necessary to determine the individual aggregation equilibrium constants and rate constants. Determining the equilibrium constants involves measurements over a concentration range in which the

**Fig. 1** The transition moment of an aggregate is at higher energy because of the electrostatic repulsion to additional cations



relative aggregation concentrations vary. In practice, this concentration range is of the order of magnitude of  $10^{-5}$  to  $10^{-3}$  M, a concentration so dilute that the only practical analytical tool is UV-vis spectroscopy. Accordingly, the enolates studied generally contain a phenyl or biphenyl ring to provide a useful chromophore for measurements. Two general tools were discovered to be effective in this study:

1. The UV-vis spectrum of some enolates was found to vary as a function of concentration, indicating that different aggregates have different spectra [9].
2. Coupled equilibria: the proton-transfer equilibria to monomeric indicators are skewed by aggregation [10].

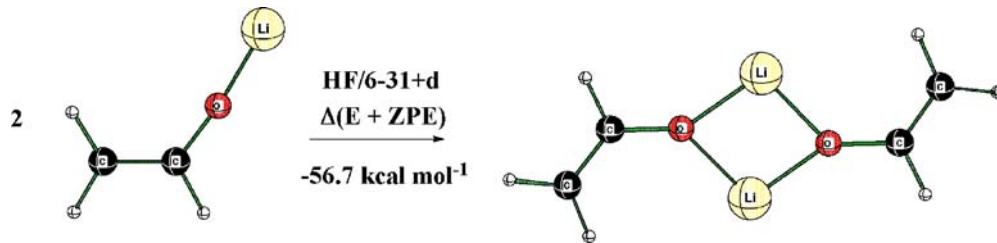
In applying the first method, a series of spectra were taken over a more than tenfold concentration range and the

digitized data were subjected to Singular Value Decomposition, SVD, a method that involves a matrix diagonalization to give a series of vectors and associated coefficients [11]. The first vector represents the mean of the spectra and has a large coefficient. The second is the first order deviation from the mean and has a significant but smaller value. The remaining coefficients are much smaller and represent noise. The two significant vectors suggest two components. In many cases the existence of an isospestic point also points to two components. From further matrix manipulation, the spectra of the two components can be determined. When each experimental spectrum is analyzed in terms of these component spectra, the composition is given. For a monomer–dimer mixture a plot of [dimer] vs [monomer]<sup>2</sup> gives a straight line whose slope is  $K_{1,2}$ ; for a monomer–tetramer mixture the corresponding plot is of [tetramer] vs [mono-

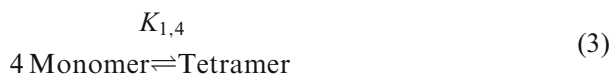
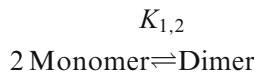
**Table 1** Aggregation of some lithium enolates in THF

Entry	Li Enolate	$K_{1,2}$	$K_{1,4}$	[M] in 1 M	pK
1			5.0E+8	0.0047	15.9
2		4300		0.011	12.6
3			4.7E+10	0.0015	14.2
4		2650		0.014	11.1
5		3800		0.011	14.0
6		1400		0.019	16.7

**Fig. 2** Dimerization of lithium vinyloxide at HF/6-31+G\* as  $\Delta E$  plus unscaled ZPE

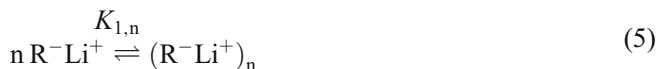


mer]<sup>4</sup>. The corresponding linear relation establishes the nature of the equilibrium (Eqs. 2 and 3).



We have found the spectrum of the aggregate always to have  $\lambda_{\max}$  at shorter wavelength than the monomer. We interpret this effect simply on the basis of Fig. 1. The transition involves movement of electron density from the oxide anion to the organic moiety. Such movement is electrostatically more difficult for an aggregate with more Li<sup>+</sup> cations close to the negative charge.

The second method is based on the proton-transfer equilibrium in Eq. 4 in which Ind-H is an indicator whose lithium salt is known to be monomeric. This equilibrium is skewed to the right by aggregation of R<sup>-</sup>Li<sup>+</sup> (Eq. 5).



The equilibrium constant defined by Eq. 6 is equivalent to the relative ion pair pK (Eq. 7). The symbol {R<sup>-</sup>Li<sup>+</sup>} is used to denote the formal concentration of R<sup>-</sup>Li<sup>+</sup> as given, for example, by spectroscopy.



$$\text{p}K_{\text{obs}}(\text{RH}) = \text{p}K(\text{Ind} - \text{H}) - \log K_{\text{obs}} \quad (7)$$

We have determined the pK's of a number of such indicators relative to the assumed value of 22.9 for fluorene, the per-hydrogen pK in DMSO [12].

Summed over the full set of aggregates in a lithium enolate equilibrium,  $K_{\text{obs}}$  is given by the expression in Eq. 8 [11]. In turn, this equation reduces to Eq. 9 for a simple monomer–dimer equilibrium and to Eq. 10 for a monomer–tetramer equilibrium. In Eq. 9, for example, a plot of  $K_{\text{obs}}$

vs {R<sup>-</sup>Li<sup>+</sup>} /  $K_{\text{obs}}$  gives a straight line from which  $K_o$  and  $K_{1,2}$  can be derived from the intercept and slope.

$$K_{\text{obs}} = \sum n K_{1,n} K_o^n \left( \{\text{R}^- \text{Li}^+\} / K_{\text{obs}} \right)^{n-1} \quad (8)$$

$$K_{\text{obs}} = K_o + 2 K_{1,2} K_o^2 \left( \{\text{R}^- \text{Li}^+\} / K_{\text{obs}} \right) \quad (9)$$

$$K_{\text{obs}} = K_o + 4 K_{1,2} K_o^4 \left( \{\text{R}^- \text{Li}^+\} / K_{\text{obs}} \right)^3 \quad (10)$$

For enolates in which both methods could be applied, the results are generally in good agreement. These methods have been applied to a range of lithium enolates [13–21]. A few of the values obtained are summarized in Table 1. One important generalization from these results is that substitution in the  $\alpha$ -position results in reduced aggregation. This generalization can be seen by comparison of entries 1 with 2 in Table 1 and of entry 3 with 4–6.

A simple ab initio model of enolate dimerization is shown in Fig. 2.

The reaction is strongly exothermic, as expected electrostatically for the union of two ion pairs, but this picture is misleading because no role is assigned to solvent. The aggregation of the lithium salt of *p*-phenylisobutyrophenone (LiPhIBP) is almost independent of temperature (Table 2), indicating that the primary driving force is entropic rather than enthalpic [16]. This had been shown previously by others, notably Jackman for lithium phenolates [22] and Chabanal for other 1:1 salts [23]. When the coordinated solvent is included with tetracoordinated lithium cations, the aggregation equilibria become Eqs. 11 and 12 (in which S is the solvent, generally THF).

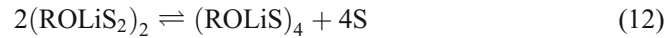


**Table 2** Effect of temperature on the aggregation of the lithium enolate of *p*-phenylisobutyrophenone (LiPhIBP);  $\Delta H^\circ=1.5\pm1$  kcal mol<sup>-1</sup>,  $\Delta S^\circ=40\pm5$  e.u. [16]

Temp. °C	$K_{1,4} M^{-3}$
25.0	$5.2 \times 10^7$
0.0	$4.4 \times 10^7$
-20.0	$3.2 \times 10^7$

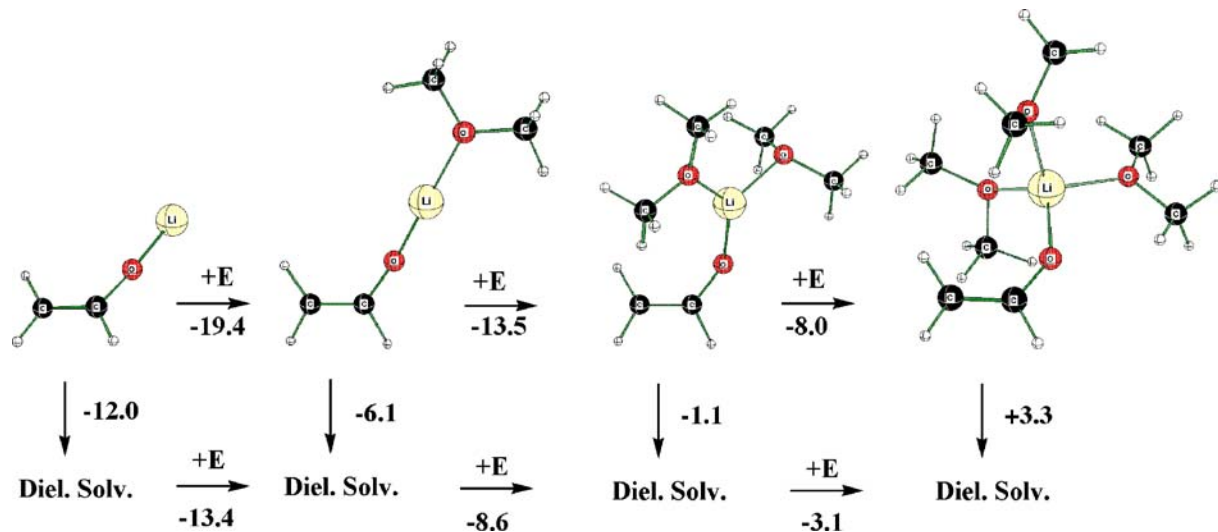


**Fig. 3** Effect of successive solvation of lithium vinyloxide by dimethyl ether ( $E$ ), HF/6-311+G\*,  $\Delta E +$  unscaled ZPE (kcal mol $^{-1}$ ), as a combination of coordination and electrostatic interaction with the dielectric continuum using the dielectric constant of THF [25]

In each case lithium remains coordinated to four oxygens, giving only a small enthalpic change but aggregation liberates solvent molecules with their increased entropy.

In computations, dimethyl ether has frequently been used in place of THF because of its smaller size [24, 25]. The effect of solvation by dimethyl ether is summarized in Fig. 3.

We considered solvation as two specific components. One is the specific coordination of solvent with lithium cation and computed as the “supermolecule” with the coordinated solvent specifically included in the molecule. The second component is the “dielectric solvation” of the coordinated species, the electrostatic interaction of the

supermolecule with a “Polarized Continuum” dielectric as included in the Gaussian program using the dielectric constant of THF [26]. Coordination is a significant exothermic term but is smaller with successive coordinations. This effect is consistent with a simple electrostatic model of interaction of the solvent dipole with the cationic charge. The successive coordinations involve the additional electrostatic interactions with the opposing dipoles of the preceding solvents. The dielectric term is initially important but rapidly diminishes with successive solvation. The first complex is a dipole whose electrostatic interaction with the dielectric is significant. As successive solvent is added, the resulting dipole moments are smaller. Further-

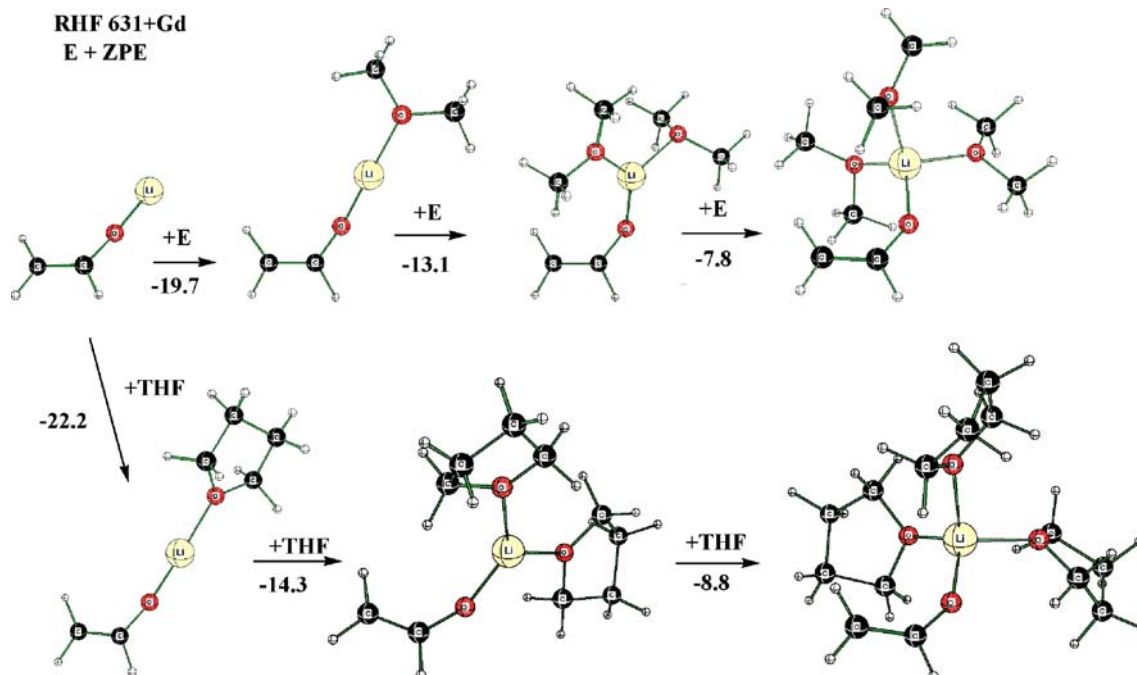
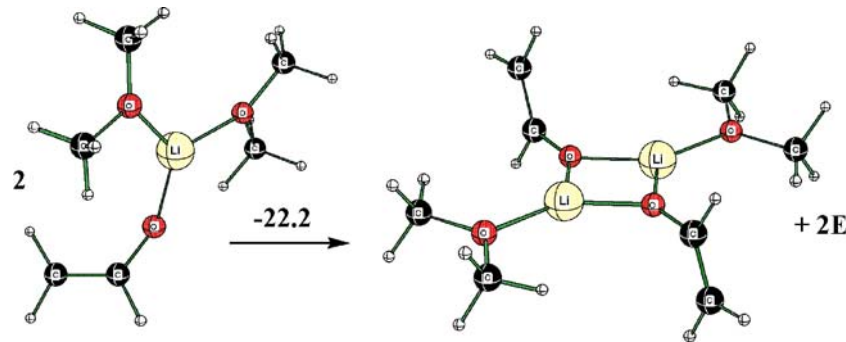


**Fig. 4** Comparison of successive coordination by dimethyl ether and THF; energy changes in kcal mol $^{-1}$

**Fig. 5** Effect of solvation on dimerization of lithium vinyl-oxide at HF/6-31+G\* + unscaled ZPE, kcal mol<sup>-1</sup>



more, the increasing size of the solvated moiety requires a greater cavity in the continuous dielectric until at the final structure the electrostatic term is insufficient to compensate for the cavity required. The net energy change for the final coordination of solvent,  $-3.1 \text{ kcal mol}^{-1}$ , is small and interesting. Chabanal [23] has suggested that the entropy change of such a reaction be approximated by the entropy of freezing of the solvent; for THF this quantity is  $-12.4 \text{ e.u.}$  which is equivalent at room temperature to an enthalpy change of  $3.7 \text{ kcal mol}^{-1}$ ; that is, the last coordination in Fig. 2 has a  $\Delta G^\circ$  of about 0 or  $K \approx 1$ . This means that the lithium enolate is not fully coordinated in solution—substantial populations are apparently tricoordinated. Because of the relatively small role of dielectric solvation in these systems we have not generally computed this term and have focused the computed models on the role of coordination solvation.

We tested how well dimethyl ether works as a computational model for THF by calculating the energetics of successive THF coordination of lithium vinyloxide compared to Me<sub>2</sub>O at the smaller basis set level of 6-31+G\*; we had shown previously that this is as effective a level as the larger 6-311+G\* for many purposes [25]. The comparison shown in Fig. 4 shows that THF is generally more coordinating than Me<sub>2</sub>O but only by about  $1 \text{ kcal mol}^{-1}$ . Even this difference is expected to be reduced by the lower dielectric solvation of THF's larger cavity size.

The effect of solvation on dimerization of lithium vinyloxide is summarized in Fig. 5. Coordination about lithium has been kept constant in the process shown. Dimerization is now much less exothermic than the uncoordinated model in Fig. 2 and would be less exothermic if the monomer has greater coordinative solvation than the dimer.

Having determined a number of aggregation equilibrium constants, we can now look at the kinetics. Kinetic measurements were made using the UV spectra of the enolates, which were therefore at low concentration, typically  $10^{-3}\text{--}10^{-4} \text{ M}$ , much less than the concentrations of the alkyl halides used, typically about  $0.02 \text{ M}$ . The second-order reactions are thus of pseudo-first order. Moreover, the reactions were typically allowed to run to only about 10% in order to avoid possible complications with mixed aggregates involving the reaction products. Under these conditions the  $\ln(\text{fraction reaction}) \approx (\text{fraction reaction})$  and it was only necessary to plot the extent

reaction vs time to determine the pseudo-first-order rate constants. These numbers were divided by the concentration of the alkyl halide to obtain the corresponding second-order rate constant. These rate constants are composites since the alkylation reaction is an S<sub>N</sub>2 process with all of the various aggregates present. For example, for a monomer–dimer system, the total rate is given by Eq. 13, which can be rearranged to Eq. 14. In these equations the  $k$ 's are the appropriate second-order rate constants.

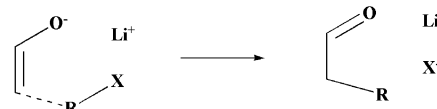
$$\text{Rate}/[\text{RX}] = k_M[\text{Monomer}] + k_D[\text{Dimer}] \quad (13)$$

$$\text{Rate}/[\text{RX}][\text{Dimer}] = k_M[\text{Monomer}]/[\text{Dimer}] + k_D \quad (14)$$

Since the aggregation equilibrium constant is known, we can calculate [Monomer] and [Dimer] at any given concentration of {Li enolate}. Eq. 14 has the convenient form that a plot of the rate quantity on the left vs [Monomer]/[Dimer] should give a straight line with slope  $k_M$  and intercept  $k_D$ . Many examples of such treatments have given normal values of  $k_M$  and values for  $k_D$  (or  $k_T$ ) of essentially zero. For these cases, a simple plot of Rate/[RX] vs [Monomer] gives a normal straight line without any upward curvature indicative of a role for  $k_D$  or  $k_T$ .

For the alkylation of the lithium enolate of *p*-phenylsulfonylisobutyrophenone (LiSIBP) with *p*-*t*-butylbenzyl bromide, a complete analysis was possible to give  $k_M=0.33 \text{ M}^{-1}\text{s}^{-1}$  and  $k_D=1.1\times 10^{-4} \text{ M}^{-1}\text{s}^{-1}$  or  $k_M/k_D=3,000$

#### S<sub>N</sub>2 Monomer



#### S<sub>N</sub>2 Dimer

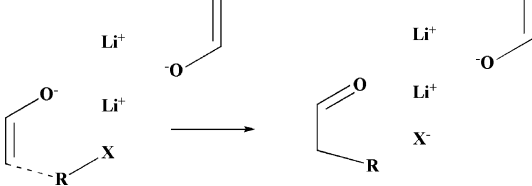
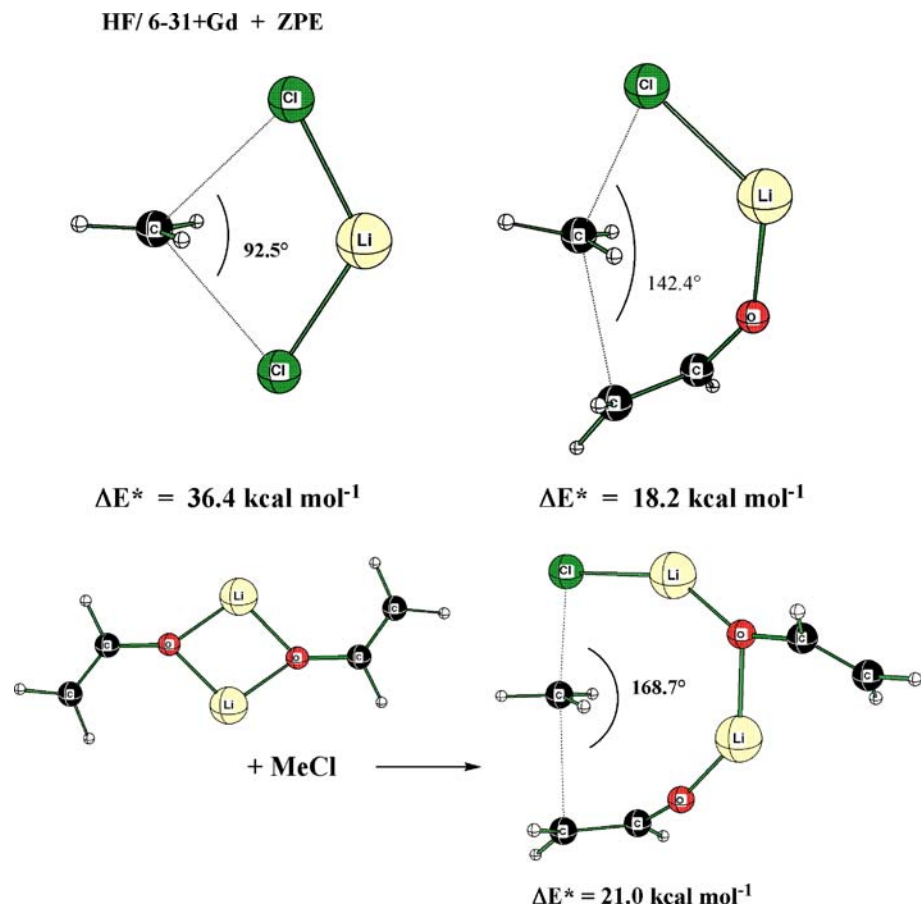


**Fig. 6** Assumed cyclic transition structure models for alkylation of lithium enolates

**Fig. 7** Computational models for some ion pair S<sub>N</sub>2 reactions



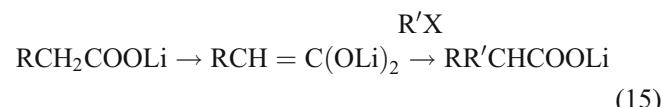
[14]. The general finding is that the monomers are much more reactive in alkylation reactions than the aggregates. This behavior was rationalized on the basis of the assumed cyclic transition structures in Fig. 6.

The S<sub>N</sub>2 reaction of the dimer is then expected to be slower because the oxide ion is neighbor to two lithium cations and is therefore less nucleophilic and the lithium cation is close to two oxide ions and is therefore less electrophilic. This hypothesis was tested by *ab initio* computations, as summarized in Fig. 7.

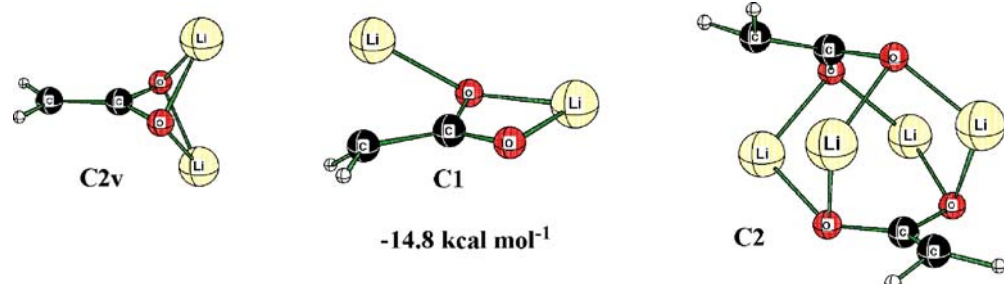
These are ion-pair S<sub>N</sub>2 reactions and simple such reactions of methyl halides with alkali halides were shown previously to have strongly bent reaction angles and consequently high reaction barriers [27]. The computed transition structure for reaction of lithium vinyloxide with methyl chloride is that of a six-membered ring with an expanded reaction bond angle and a much lower and more

accessible reaction barrier. The corresponding reaction of the dimer has broken one Li–O coordination bond with a correspondingly larger and almost normal reaction bond angle; nevertheless, the loss of coordination results in a substantially higher reaction barrier.

Reactions of dilithiated carbonyl compounds have achieved great importance in synthetic chemistry. For example, substituted acetic acids can usually be dimetalated to the dilithium enediolates, which can then be alkylated to give the corresponding disubstituted acetic acids cleanly (Eq. 15).



**Fig. 8** Computed structures for unsolvated monomer and dimer of CH<sub>2</sub>=C(OLi)<sub>2</sub> at HF/6-31+G\*. The C1 structure of the monomer is 14.8 kcal mol<sup>-1</sup> more stable than the C2v structure



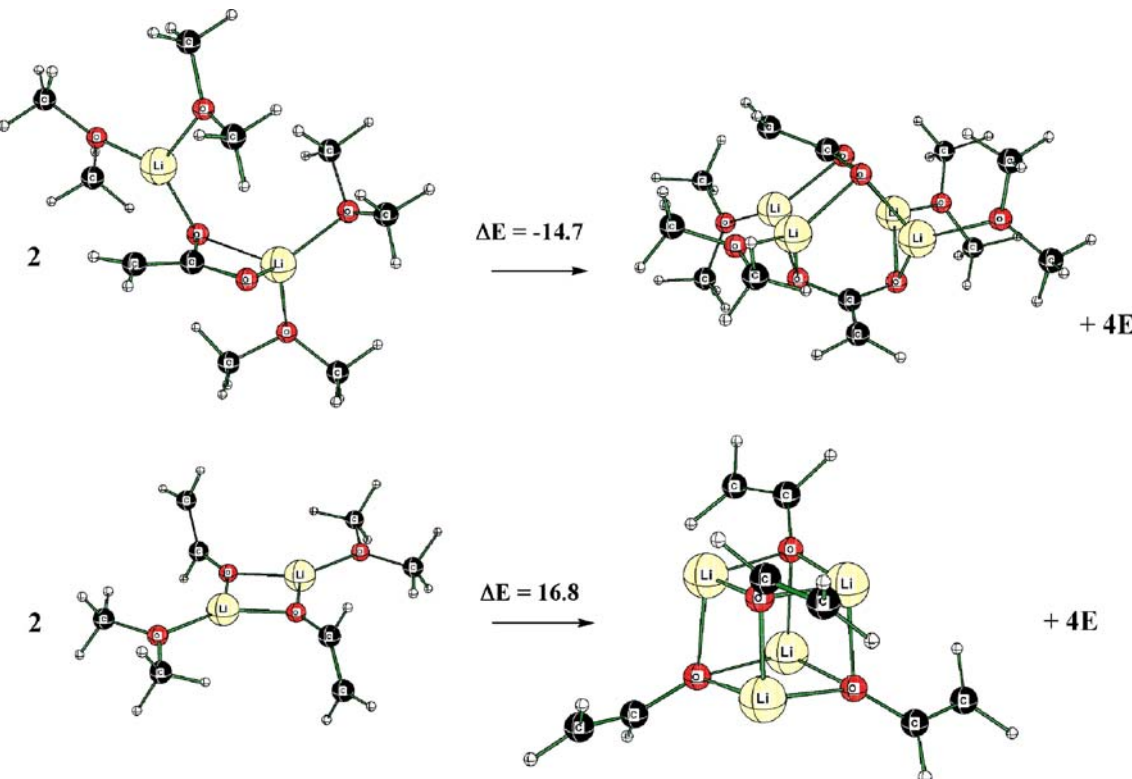


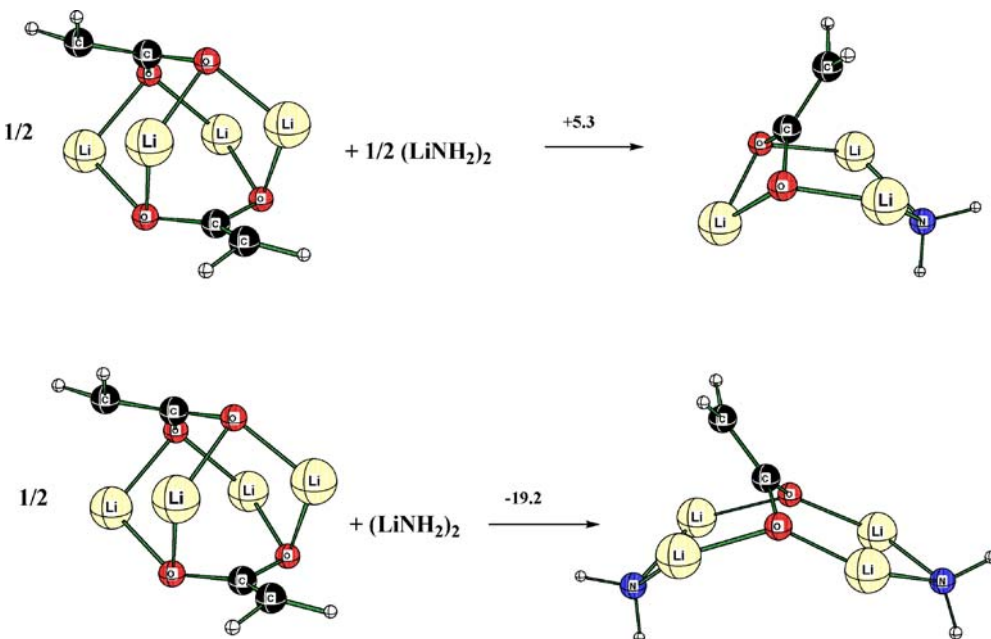
**Fig. 9** Computed dimerization reactions at HF/6-31+G\* with lithium solvated such that the same numbers of dimethyl ethers are liberated. Energy changes shown are kcal mol<sup>-1</sup>

In earlier work, the dilithium salt of  $\alpha$ -naphthylacetic acid was found to be aggregated and to have a  $pK$  of about 23 [28]. The spectrum does not change with concentration and lithium carboxylates themselves are aggregated, so neither of our two general methods could be used to determine the extent of aggregation. The aggregates are broken up with hexamethylphosphoramide (HMPA), how-

ever, and the stoichiometry indicates the dilithium salt to be a dimer [29]. This dimer is exceptionally tight and the amount of monomer present is too small to show up in alkylation kinetics.

Ab initio modeling at the HF/6-31+G\* level showed two minima on the potential energy surface for the unsolvated dilithium salt of acetic acid, a C<sub>2</sub>v structure and a

**Fig. 10** Computed energetics of some equilibria with dilithium enediolate to give mixed aggregates with lithium amide. Energy changes in kcal mol<sup>-1</sup> indicate that lithium amide forms 2:1 mixed aggregates



lower energy C1 structure as shown in Fig. 8. The corresponding dimer has a structure that resembles a distorted cubic structure of a lithium enolate tetramer. The dimerization of  $\text{CH}_2=\text{C}(\text{OLi})_2$  was found to be much more exothermic than that of  $\text{CH}_2=\text{CHLi}$  dimer going to tetramer (Fig. 9). In both cases the lithiums were coordinatively solvated to the same degree such that the same numbers of ethers were liberated in the reaction. The computed energetics are in good qualitative agreement with the experimental chemistry.

Dilithium  $\alpha$ -naphthylacetate was found to form mixed aggregates with some lithium amides but the stoichiometry was not determined. Computed structures and reactions summarized in Fig. 10 suggest that the amides form 2:1 complexes with the dilithium enediolate.

The molecular orbital computations were accomplished with various versions of the Gaussian program up to Gaussian 03 [26].

**Acknowledgements** In the period since I became Emeritus in 1993, a large group of undergraduate and graduate students and post-doctoral coworkers have done experimental and computational research in this project: (in alphabetical order) Alessandro Abbotto, Godwin S-C Choy, Jayasree Elambalassery, Antonio Facchetti, Rustram Gareyev, Faraj Hasanayn, Marc Husemann, Kathleen V. Kilway, Yeong-Joon Kim, James A. Krom, Simon S-W Leung, Joe C-Y Liang, Arlene McKeown, James Pugh, Manolis Stratakis, and Daniel Z-R. Wang. Two contributing visitors were Prof. Eusabio Juaristi and Prof. Larry M. Pratt. This work was assisted by grants from the National Science Foundation and the National Institutes of Health.

## References

- Evans DA, Nelson JV, Taber TR (1982) Topics in Stereochemistry 13:1–115
- Mukaiyama T (1982) Org React 28:203–331
- Heathcock CH (1991) In: Comprehensive organic synthesis, vol 1. Pergamon, Oxford, pp 181–238
- Braun M (1992) Advances in carbanion chemistry, vol 1. Jai, Greenwich CT, pp 177–247
- Arya P, Qin H (2000) Tetrahedron 56:917–947
- Wen JQ, Grutzner JB (1986) J Org Chem 51:4220, Seebach D (1988) Angew Chem Int Ed Engl 27:1624–1654, Boche G (1989) Angew Chem Int Ed Engl 28:277, Arnett EM, Moe KD (1991) J Am Chem Soc 113:7288–7293, Jackman LM, Bortiatynski J (1992) Adv Carbanion Chem 1:45–87
- Seebach D, Amstutz R, Dunitz JD (1981) Helv Chim Acta 64:2622–2626, Williard PG, Hintze MJ (1990) J Am Chem Soc 112:8602–8604, Bach RD, Andres JL, Davis FA (1992) J Org Chem 57:613, Juaristi E, Beck AK, Hansen J, Matt T, Mukhopadhyay T, Simson M, Seebach D (1993) Synthesis 1271, Wei Y, Bakthavatchalam R (1993) Tetrahedron 49:2373–2390, Solladie-Cavallo A, Csaky AG, Gantz I, Suffert J (1994) J Org Chem 59:5343–5346
- Seeman JI (1983) Chem Rev 83:83–134
- Ciula JC, Streitwieser A (1992) J Org Chem 57:431–432, correction p 668
- Kaufman MJ, Streitwieser A (1987) J Am Chem Soc 109: 6092–6097
- Krom JA, Petty JT, Streitwieser A (1993) J Am Chem Soc 115: 8024–8030
- Streitwieser A, Wang DZ, Stratakis M, Facchetti A, Gareyev R, Abbotto A, Krom JA, Kilway KV (1998) Can J Chem 76:765–769
- Abbotto A, Streitwieser A (1995) J Am Chem Soc 117:6358–6359
- Abu-Hasanayn F, Stratakis M, Streitwieser A (1995) J Org Chem 60:4688–4689
- Gareyev R, Ciula JC, Streitwieser A (1996) J Org Chem 61: 4589–4593
- Abbotto A, Leung S S-W, Streitwieser A, Kilway KV (1998) J Am Chem Soc 120:10807–10813
- Streitwieser A, Wang DZ-R (1999) J Am Chem Soc 121:6213–6219
- Wang DZ-R, Streitwieser A (1999) Can J Chem 77:654–658
- Wang DZ-R, Kim Y-J, Streitwieser A (2000) J Am Chem Soc 122:10754–10760
- Streitwieser A, Kim Y-J, Wang DZ-R (2001) Org Lett 3:2599–2601
- Wang DZ, Streitwieser A (2003) J Org Chem 68:8936–8942
- Jackman LM, DeBrosse CW (1983) J Am Chem Soc 105: 4177–4184
- Chabanel M (1990) Pure & Appl Chem 62:35–46
- Abbotto A, Streitwieser A, Schleyer PvR (1997) J Am Chem Soc 119:11255–11268
- Pratt LM, Streitwieser A (2003) J Org Chem 68:2830–2838
- Frisch MJ, Trucks GW, Schlegel HB, Scuseria GE, Robb MA, Cheeseman JR, Montgomery JA, Vreven T, Kudin KN, Burant JC, Millam JM, Iyengar SS, Tomasi J, Barone V, Mennucci B, Cossi M, Scalmani G, Rega N, Petersson GA, Nakatsuji H, Hada M, Ehara M, Toyota K, Fukuda R, Hasegawa J, Ishida M, Nakajima T, Honda Y, Kitao O, Nakai H, Klene M, Li X, Knox JE, Hratchian HP, Cross JB, Adamo C, Jaramillo J, Gomperts R, Stratmann RE, Yazyev O, Austin AJ, Cammi R, Pomelli C, Ochterski JW, Ayala PY, Morokuma K, Voth GA, Salvador P, Dannenberg JJ, Zakrzewski VG, Dapprich S, Daniels AD, Strain MC, Farkas O, Malick DK, Rabuck AD, Raghavachari K, Foresman JB, Ortiz JV, Cui Q, Baboul AG, Clifford S, Cioslowski J, Stefanov BB, Liu G, Liashenko A, Piskorz P, Komaromi I, Martin RL, Fox DJ, Keith T, Al-Laham MA, Peng CY, Nanayakkara A, Challacombe M, Gill PMW, Johnson B, Chen W, Wong MW, Gonzalez C, Pople JA (2003) Gaussian 03, Revision B.05. Gaussian Inc, Pittsburgh PA
- Harder S, Streitwieser A, Petty JT, Schleyer PvR (1995) J Am Chem Soc 117:3253–3259
- Gronert S, Streitwieser A (1988) J Am Chem Soc 110:4418–4419
- Streitwieser A, Husemann M, Kim Y-J (2003) J Org Chem 68:7937–7942